Prognostic value and underlying mechanism of autophagy-related genes in bladder cancer

Keying Zhang
Department of Urology, Xijing Hospital
Jingwei Wang
Department of Medicine Chemistry and Pharmaceutical Analysis, School of Pharmacy
Chao Xu
Department of Urology, Xijing Hospital
Jingliang Zhang
Department of Urology, Xijing Hospital
Shaojie Liu
Department of Urology, Xijing Hospital
Xiang Zhou
State Key Laboratory of Cancer Biology, Department of Immunology
Xiaolong Zhao
Department of Urology, Xijing Hospital
Shiyuan Peng
Department of Urology, Xijing Hospital
Yao Jiang
Department of Urology, Xijing Hospital
Fa Yang
Department of Urology, Xijing Hospital
Jun Qin
Department of Urology, Xijing Hospital
Ping Meng
Department of Urology, Xijing Hospital
Changhong Shi
Laboratory Animal Center
Rui Zhang
State Key Laboratory of Cancer Biology, Department of Immunology
An-Gang Yang
State Key Laboratory of Cancer Biology, Department of Immunology
Donghui Han
Department of Urology, Xijing Hospital
Weihong Wen
Institute of Medical Research
Weijun Qin (qinwj@fmmu.edu.cn)
Department of Urology, Xijing Hospital

Research

Keywords: Bladder cancer, Autophagy-related gene, Prognostic signature, TIICs, TME

DOI: https://doi.org/10.21203/rs.3.rs-74759/v1

Abstract

Background

Bladder cancer (BLCA) is the most common malignancy whose early diagnosis can ensure better prognosis. However, the predictive accuracy of commonly used predictors, including patients' general condition, histological grade and pathological stage, is insufficient to identify the patients who need invasive treatment. Autophagy is regarded as a vital factor in maintaining mitochondrial function and energy homeostasis in cancer cells. Whether autophagy-related genes (ARGs) can predict the prognosis of BLCA patients deserves to be investigated.

Methods

Based on BLCA data retrieved from the Cancer Genome Atlas (TCGA) and ARGs list obtained from the Human Autophagy Database (HADb) website, we identified prognosis-related differentially expressed ARGs (PDEARGs) through Wilcox text and constructed a PDEARGs-based prognostic model through multivariate Cox regression analysis. The predictive accuracy, independent forecasting capability, and the correlation between present model and clinical variables or tumor microenvironment (TME) were evaluated through R software. Enrichment analysis of PDEARGs was performed to explore the underlying mechanism, and a systematic prognostic signature with nomogram was constructed by integrating clinical variables and aforementioned PDEARGs-based model.

Results

We identified several PDEARGs and constructed a PDEARGs-based prognostic model, which could precisely predict the prognosis of BLCA patients. Then, we found that the risk score generated by PDEARGs-based model could effectively reflect deteriorated clinical variables and tumor-promoting microenvironment. Additionally, several immune-related gene ontology (GO) terms were significantly enriched by PDEARGs, which might provide insights for present model and propose potential therapeutic targets for BLCA patients. Finally, a systematic prognostic signature with promoted clinical utility and predictive accuracy was constructed to assist clinician decision.

Conclusion

PDEARGs are valuable prognostic predictor and potential therapeutic targets for BLCA patients.

Background

Bladder cancer (BLCA) is the most common malignancy of the urinary system with about 549,000 new cases and 200,000 death worldwide in 2018 [1]. BLCA is characterized by high rate of recurrence and progression, which impose a considerable economic burden on healthcare system and have substantial effects on the quality of life and overall outcome of BLCA patients. Although novel treatments for BLCA have been proposed, such as immunotherapy of PD-1/PD-L1 [2], the five-year survival rate for advanced/metastatic BLCA is only 15% and the median overall survival is less than 15 months [3]. Early diagnosis and recurrence monitoring of BLCA would be valuable for better prognosis. However, the predictive accuracy of commonly used predictors, including patients' general condition, histological grade and pathological stage, is insufficient to identify the patients who need invasive treatment [4]. Recently, biomarker-based signature is regarded as a promising tool to predict the prognosis of BLCA patients and assist clinical decision [5].

Autophagy is a highly conserved cellular self-degradative process. Some cancers could use autophagy-mediated recycling to maintain mitochondrial function and energy homeostasis to meet their elevated metabolic demand of growth and proliferation [6]. Therefore, autophagy-based prognostic signature has been widely investigated, and autophagy inhibition has been proposed as a novel cancer therapy strategy [7]. As reported, autophagy-related genes (ARGs) can effectively select high-risk colorectal cancer patients who require more aggressive therapeutic interventions [8]. Liu et al. constructed a 22-ARGs-based signature that could dichotomize patients with significantly different overall survival (OS) and independently predict the OS in TCGA lung

adenocarcinoma [9]. The predictive value of ARGs-based signature has also been validated in glioblastoma [10] and breast cancer [11]. However, the clinical relevance and prognostic significance of ARGs-based signature in BLCA remain unknown.

In present study, we aimed to develop a reliable prognostic model for BLCA patients using multiple ARGs and investigate its clinical implications. Furthermore, we evaluated the correlation between present prognostic model and tumor microenvironment (TME), and explored the underlying mechanism. Finally, to facilitate clinical utility of the aforementioned model, a systematic prognostic signature was constructed by integrating clinical predictors and ARGs-based molecular biomarkers.

Methods

Data source and preprocessing

Transcriptomic data (RNA-Seq FPKM) and clinical information were downloaded from the Cancer Genome Atlas (TCGA) portal (https://portal.gdc.cancer.gov/), including 413 BLCA data and 19 non-tumor data. After integrating those data through ID numbers, replicate probes were replaced with their average via limma package [12]. Patients with follow-up time < 90 d or other incomplete data were removed. All data were processed and analyzed with R software (https://www.r-project.org/), and flow diagram of present study was shown in Fig. 1.

Differential expression analysis and ARGs identification

DEGs between tumor tissues and normal tissues were analyzed through Wilcoxon test. p-value was adjusted with FDR, and filter criteria was FDR < 0.05 and $|\log_2$ fold-change [FC]$|$ > 1. DEARGs were identified by matching the DEGs with a latest list of ARGs obtained from the Human Autophagy Database (HADb) website (http://www.autophagy.lu/index.html). Univariate Cox regression analysis was used to identify possible PDEARGs (P < 0.05).

Prognostic signature construction and validation

Multivariate Cox regression analysis was adopted to construct a PDEARGs-based prognostic model, and the risk score of each patient was calculated using the following formula [13]:

$$\text{Risk score} = \sum_{i=1}^{n} \text{coefficient (gene i)} * \text{Expression value of (gene i)}$$

Individuals were separated into high-risk or low-risk groups according to median risk score. Subsequently, survival analysis and receiver operating characteristic (ROC) analysis were performed as reported [5]. The expression level of the five selected PDEARGs between two risk groups was analyzed with R software as well.

Independent prognostic factors analysis

Univariate Cox regression analysis was performed to identify factors affecting the OS of BLCA patients and multivariate Cox regression analysis was used to evaluate whether the risk score generated from present prognostic model was capable to be used as an independent prognostic factor. P < 0.05 was considered statistically significant.

Clinical utility of prognostic signature

The relationship between risk factors of present model and certain clinical variables (i.e. age, gender, histological grade, pathological stage and tumor-node-metastasis (TNM) status) was analyzed with t-test. The box plot was prepared with beeswarm R package and the impact of PDEARGs on BLCA prognosis was analyzed through survival R package.

Correlation between risk score and TME

Tumor purity, infiltrating stromal and immune cells of TCGA-BLCA were assessed through ESTIMATE R package as previously reported [14]. The relative fraction of 22 TIICs types in each sample was quantified by CIBERSORT method and LM22 signature matrix [15, 16]. The algorithm ran at 100 permutations with a threshold of P < 0.05 to select eligible patients for further analysis

[17]. The correlation between risk score and TME was analyzed with the Pearson correlation coefficient test, and the impact of TME on clinical variables was evaluated as well.

Enrichment analysis of PDEARGs

GO function enrichment of the five selected PDEARGs was performed via clusterProfiler and enrichplot R package. FDR < 0.05 was considered statistically significant. To better explain the relationship between PDEARGs and GO terms, a chord plot was constructed with Goplot R package.

Construction and validation of PDEARGs-based systematic prognostic signature

A systematic prognostic signature was constructed through multivariate Cox regression by integrating seven clinical variables (i.e. age, gender, histological grade, pathological stage, and TNM status) with aforementioned five PDEARGs-based signatures. The variables that were highly correlated with others was deleted to avoid overfitting. The median of the systematic risk was used to separate the patients into two risk groups and survival probability was analyzed using R software. Predictive accuracy of the novel systematic signature was evaluated with survivalROC R package. Finally, the systematic signature was visualized through a nomogram constructed by rms R package.

Results

Identification of BLCA specific PDEARGs

We obtained 3126 differentially expressed genes (DEGs) based on TCGA-BLCA dataset, among which 1223 genes were downregulated and 1903 genes were upregulated in tumor tissues compared with normal tissues (false discovery rate (FDR) < 0.05, $|\log_2 FC| > 1$; Fig. 2a). Then, 34 BLCA-specific differentially expressed ARGs (DEARGs) were identified (Fig. 2b), and five prognostic DEARGs (PDEARGs) were found to be significantly associated with the OS of BLCA patients ($P < 0.05$; Fig. 2c). Among the five PDEARGs, *APOL1* with hazard ratio ≤ 1 was regarded as a protective gene, while the other four genes (*DIRAS3*, *NAMPT*, *P4HB*, and *SPHK1*) were identified as high-risk genes predicting a poor prognosis of BLCA.

Construction and validation of prognostic signature

Multivariate Cox regression was employed to construct a five PDEARGs-based prognostic risk model (Table 1). Subsequently, the risk score for each patient was calculated with the following computational formula:

Risk score = (-0.0019 × expression of *APOL1*) + (0.0775 × expression of *DIRAS3*) + (0.0127 × expression of *NAMPT*) + (0.0030 × expression of *P4HB*) + (0.0120 × expression of *SPHK1*).

Individuals were sorted into high-risk group (n = 185) and low-risk group (n = 186) by the median risk score 1.02. Survival analysis indicated that the prognosis was poorer in high-risk group than low-risk group ($P < 0.001$; Fig. 3a). Precisely, the five-year OS rate in high-risk group was 33.2%, while was 59.5% in low-risk group. Then, we analyzed the distribution of risk score and survival status of each patient, and a large amount of death existed in high-risk group (Fig. 3b). As well, heat map and a series of box plots were generated to depict the expression level of the five selected PDEARGs, among which the protective gene (*APOL1*) was downregulated, and the other four risk genes were upregulated in patients with high-risk score (Fig. 3b and d). The area under the curve (AUC) was 0.724, which was much higher than other clinical parameters, suggesting that present model was more accurate in predicting OS of BLCA patients (Fig. 3c).

Independent prognostic value of present signature

As shown in Fig. 4a, the variables of pathological stage, tumor-node-metastasis (TNM) status, and risk score were associated with the prognosis of BLCA patients ($P < 0.05$). Multivariate analysis showed that the risk score was an independent prognostic factor for OS ($P < 0.01$; Fig. 4b). The hazard ratio for risk score was 1.695, indicating that high risk score would predict a bad prognosis. The commonly used clinical variables, such as age, gender, pathological stage, and TNM status were not sufficient to serve as independent prognostic predictors ($P > 0.05$).

Clinical utility of present signature

The relationship between present model and clinical variables were analyzed (Table 2). High-expression of *APOL1* was associated with decreased pathological stage, N status and M status ($P < 0.05$; Fig. 5b-d). Contrarily, as the value of risk score or the expression of the other four genes (*DIRAS3*, *NAMPT*, *P4HB*, and *SPHK1*) increased, the histological grade, pathological stage, T status and/or N status of BLCA patients increased ($P < 0.05$; Fig. 5e-u). Furthermore, low-expression of *APOL1* and increased risk score were observed in patients with age > 65 ($P < 0.05$; Fig. 5a-q). Survival analysis showed that high-expression of the protective gene *APOL1* indicated a good prognosis ($P < 0.01$; Fig. 6a), while high-expression of risk gene *P4HB* resulted in a poor prognosis ($P < 0.05$; Fig. 6d). The other three risk genes (*DIRAS3*, *NAMPT*, and *SPHK1*) had no significant effect on survival outcome ($P > 0.05$; Fig. 6b, c and e).

Correlation between risk score and TME

As shown in Fig. 7a-d, with the increase of risk score generated by present prognostic signature, tumor infiltrating stromal cells (i.e. stromal score) and estimate score (sum of stromal score and immune score) significantly increased, meanwhile tumor purity significantly decreased ($P < 0.05$). Additionally, 22 types of tumor-infiltrating immune cells (TIICs) in TCGA-BLCA were analyzed with CIBERSORT, and the content of neutrophils, macrophages M0 and M2 increased with risk score ($P < 0.05$; Fig. 7e-h). Furthermore, a high proportion of macrophages M0 could lead to a poor prognosis, accompanied with increased pathological stage, N status and M status of BLCA patients ($P < 0.05$; Fig. 7i-l).

GO enrichment analysis

Gene Ontology (GO) enrichment analysis showed that the five selected PDEARGs were associated with 52 biological processes (BPs), six molecular functions (MFs), and nine cellular components (CCs), among which immunologic process related GO terms were significantly enriched, such as the activation of microglial cell, leukocyte and macrophage as well as inflammatory response. Besides, oxidative stress and relevant apoptotic signal pathway were significantly enriched (FDR < 0.05; Fig. 8a). To better explain the relationship between PDEARGs and GO terms, a chord plot was constructed and three key genes (ARGs *SPHK1*, *P4HB* and *NAMPT*) were founded (Fig. 8b).

Construction and validation of PDEARGs-based systematic prognostic signature

To promote clinical application and predictive accuracy of aforementioned model, we constructed a systematic prognostic signature by integrating seven clinical variables and the five PDEARGs-based signatures. The clinical variables (i.e. age, histological grade and TNM status) that correlated highly with the aforementioned risk score were deleted to avoid overfitting. Then, the systematic risk of each patient was calculated with the following computational formula (Table 3):

Systematic risk = (-0.5755 × gender) + (0.6253 × pathological stage) + (0.5276 × risk score generated from aforementioned model); gender: female = 1, male = 0.

The median of the systematic risk was 0.96, and with the increase of systemic risk, a bad prognosis of BLCA patients was observed ($P < 0.001$; Fig. 9a and c). Precisely, the three-year and five-year OS rate was 49.0% and 37.6% in high-risk group, while was 77.6% and 69.0% in low-risk group, respectively. A nomogram was constructed accordingly and the AUC value for systematic prognostic signature was 0.791, which was more accurate than pure PDEARGs-based model (Fig. 9b and d).

Discussion

BLCA is a frequent malignant disease with rising incidence and high recurrence rates [18]. Although new diagnostic and therapeutic strategies have been carried out over the past several decades, yet the clinical outcome of BLCA patients remains unsatisfied [3, 19]. Hence, there is an urging need to develop better diagnostic methods to accurately identify asymptomatic and recurrent individuals in an early stage, and to propose novel treatment targets to improve prognosis. Previous studies have revealed that autophagy plays an essential role in TME regulation, which may result in tumor cell migration and invasion, tumor stem cell maintenance and therapy resistance [20, 21]. Therefore, ARGs may be an ideal biomarker or indicator to predict the progression and prognosis of BLCA.

Recently, many malignant tumor related studies have shown that ARGs-based signature or multigene expression patterns can favorably predict cancer prognosis [8, 9, 11]. However, whether this novel prognostic signature can predict the outcome of BLCA patients aroused our interest. In present study, we identified five optimal PDEARGs based on a comprehensive analysis, among which *APOL1* was a protective gene and the other four PDEARGs were risk genes. Then, we constructed a reliable PDEARGs-based prognostic model that could stratify the TCGA-BLCA patients into two risk groups with statistically different survival outcomes. The risk score generated from the present signature could serve as an independent prognostic factor to predict patients' OS, and the predictive accuracy (AUC = 0.724) was much better than other clinical parameters. As reported, AUC > 0.60 was regarded as acceptable for predictions [22], thus, the present PDEARGs-based signature can precisely predict the prognosis of BLCA patients.

Subsequently, we analyzed the expression of the five PDEARGs in two risk groups and evaluated the relationship between present signature and certain clinical variables. Firstly, the expression of protective gene *APOL1* was downregulated in high-risk group and the other four risk genes were upregulated in patients with increased risk score. Consistently, *APOL1* expression significantly decreased with the increase of pathological stage, N and M status. The high expression of risk genes was accompanied with bad histological grade, pathological stage, TNM status and prognosis. Based on above, the present signature constructed with low-expression of protective gene and high-expression of risk genes could accurately predict the progression of BLCA patients, including histological grade, pathological stage, TNM status and survival outcome. What's more, BLCA incidence increased with age [23], and we found that *APOL1* level was down-regulated and risk score increased in elderly patients (age > 65), which further confirmed the reliability of present model.

TME, which is comprised of recruited stromal cells and TIICs, has emerged as an important player in tumor progression, with the potential to be used in future treatment and diagnosis [24]. In present study, the TME of BLCA patients was analyzed with ESTIMATE and CIBERSORT R package. With the increase of risk score generated from PDEARGs-based signature, tumor purity significantly decreased, and the proportion of stromal cells, neutrophils, and macrophage (M0 and M2 phenotypes) in tumor tissues significantly increased, which was correlated with bad pathological stage, detrimental TNM status, and poor prognosis. As reported, tumor-associated stromal cells can synthesis and secrete many pro-tumorigenic factors to promote cancer initiation, angiogenesis, invasion, and metastasis [25]. Additionally, emerging evidence indicates that elevated neutrophils are associated with detrimental outcome in several solid tumors and new strategies to decrease their presence and activity have shown efficacy in preclinical models [26, 27]. Tumor-associated macrophage (TAM) is another prominent component of TME, and the accumulation of M0 and M2 macrophages in tumors is most strongly associated with poor clinical outcome [28]. Therefore, the ability to reflect the tumor-promoting microenvironment may help to explain why present PDEARGs-based signature could precisely predict the prognosis of BLCA patients.

To explore the underlying mechanism by which present prognostic model effectively stratified BLCA patients, GO enrichment analysis of the five PDEARGs was performed and several immune-related GO terms were significantly enriched, such as macrophage activation, inflammatory response, cellular response to decreased oxygen levels and related apoptotic signaling pathway. It has been reported that ARGs are tightly related with hypoxia and hypoxia-induced metabolic reprogramming, among which *P4HB* is a key molecule has been extensively studied [6, 29]. The expression of *P4HB* has been found to significantly increase in several solid tumors including bladder cancer [30], kidney cancer [31] and prostate cancer [29], which is consistent with present study. Besides, hypoxia and oxygen stress induced autophagy and apoptosis could be regulated by ARGs such as *SPHK1*, *P4HB* and *NAMPT* [32]. During the process mentioned above, inflammatory response would be initiated and the TME could be changed to recruit and activate macrophages. *NAMPT* is regarded as a pleiotropic modulator governing monocyte/macrophage differentiation, polarization and migration [33]. Therefore, we speculate that the process of "PDEARGs → autophagy → TME change→ TAM recruitment and polarization → tumor progression" would provide insights for present prognostic signature and propose potential treatment targets for BLCA patients.

Though present prognostic model exhibits a promising value in predicting the prognosis of BLCA patients, we intend to integrate clinical variables and risk score generated from aforementioned five PDEARGs-based signatures to construct a systematic signature with promoted clinical utility and predictive accuracy. Notably, the novel systematic signature could more precisely predict the prognosis of TCGA-BLCA patients (AUC = 0.791). As reported, AUC > 0.75 was deemed to have excellent predictive value [22]. Then, a nomogram of the systematic signature was prepared for clinicians to identify BLCA patients who need invasive therapy.

Conclusions

We constructed a valuable PDEARGs-based prognostic model that can precisely predict the prognosis of BLCA patients. The risk score generated from this model can serve as an independent prognostic factor and can effectively reflect the tumor-promoting microenvironment. GO enrichment analysis revealed the underlying mechanism, which may provide insights for present model and propose potential treatment targets for BLCA patients. Additionally, a systematic signature integrating clinical variables and aforementioned five PDEARGs-based model was constructed for clinical application. Inevitably, large-scale, multi-center studies are necessary to confirm the clinical benefit of our results.

Abbreviations

BLCA: Bladder cancer; ARGs:Autophagy-related genes; OS:Overall survival; TME:Tumor microenvironment; DEGs:Differentially expressed genes; FDR:False discovery rate; DEARGs:Differentially expressed ARGs; PDEARGs:Prognostic DEARGs; AUC:Area under the curve; TNM:Tumor-node-metastasis; TIICs:Tumor-infiltrating immune cells; GO:Gene Ontology; BPs:Biological processes; MFs:Molecular functions; CCs:Cellular components; TAM:Tumor-associated macrophage; ROC:Receiver operating characteristic.

Declarations

Acknowledgements

Not applicable.

Authors' contributions

KYZ, JWW, and CX: design, analysis and interpretation of data, drafting of the manuscript, critical revision of the manuscript. KYZ, JWW, CX, JLZ, SJL, XZ, and XLZ: statistical analysis;

SYP, YJ, and FY: acquisition of data; JQ, PM, CHS, RZ, and AGY: literature search; DHH, WHW, and WJQ: critical revision of the manuscript, administrative support, obtaining funding, supervision. All authors read and approved the final manuscript.

Funding

The work has been supported by grants from the National Natural Science Foundation of China (No. 81772734, 81802935) and the Innovation Capability Support Plan of Shaanxi Province (2020PT-021). The funders had no role in study design, data collection and analysis, decision to publish, or preparation of the manuscript.

Availability of data and materials

The datasets analyzed during the current study are available in the TCGA repository (https://portal.gdc.cancer.gov).

Ethics approval and consent to participate

Not applicable

Consent for publication

Not applicable

Competing interests

The authors declare that they have no competing interests.

References

1. Bray F, Ferlay J, Soerjomataram I, Siegel RL, Torre LA, Jemal A. Global cancer statistics 2018: GLOBOCAN estimates of incidence and mortality worldwide for 36 cancers in 185 countries. CA Cancer J Clin. 2018;68:394-424.

2. Powles T, Eder JP, Fine GD, Braiteh FS, Loriot Y, Cruz C, et al. MPDL3280A (anti-PD-L1) treatment leads to clinical activity in metastatic bladder cancer. Nature. 2014;515:558-562.
3. Butt SUR, Malik L. Role of immunotherapy in bladder cancer: past, present and future. Cancer Chemotherapy & Pharmacology. 2018;81:629-645.
4. He A, He S, Peng D, Zhan Y, Li Y, Chen Z, Gong Y, Li X, Zhou L. Prognostic value of long non-coding RNA signatures in bladder cancer. Aging (Albany NY). 2019;11:6237-6251.
5. Qiu H, Hu X, He C, Yu B, Li Y, Li J. Identification and Validation of an Individualized Prognostic Signature of Bladder Cancer Based on Seven Immune Related Genes. Front Genet. 2020;11:12-24.
6. White E, Mehnert JM, Chan CS. Autophagy, Metabolism, and Cancer. Clin Cancer Res. 2015;21:5037-5046.
7. Levy J, Towers CG, Thorburn A. Targeting autophagy in cancer. Nat Rev Cancer. 2017;17:528-542.
8. Zhou Z, Mo S, Dai W, Ying Z, Zhang L, Xiang W, Han L, Wang Z, Li Q, Wang R, Cai G. Development and Validation of an Autophagy Score Signature for the Prediction of Post-operative Survival in Colorectal Cancer. Front Oncol. 2019;9:878.
9. Liu Y, Wu L, Ao H, Zhao M, Leng X, Liu M, Ma J, Zhu J. Prognostic implications of autophagy-associated gene signatures in non-small cell lung cancer. Aging (Albany NY). 2019;11:11440-11462.
10. Wang Z, Gao L, Guo X, Feng C, Lian W, Deng K, Xing B. Development and validation of a nomogram with an autophagy-related gene signature for predicting survival in patients with glioblastoma. Aging (Albany NY). 2019;11:12246-12269.
11. Gu Y, Li P, Peng F, Zhang M, Zhang Y, Liang H, Zhao W, Qi L, Wang H, Wang C, Guo Z. Autophagy-related prognostic signature for breast cancer. Mol Carcinog. 2016;55:292-299.
12. Yue C, Ma H, Zhou Y. Identification of prognostic gene signature associated with microenvironment of lung adenocarcinoma. Peerj. 2019;7:e8128-e8144.
13. Wan B, Liu B, Huang Y, Yu G, Lv C. Prognostic value of immune-related genes in clear cell renal cell carcinoma. Aging (Albany NY). 2019;11:11474-11489.
14. Yoshihara K, Shahmoradgoli M, Martínez E, Vegesna R, Kim H, Torres-Garcia W, et al. Inferring tumour purity and stromal and immune cell admixture from expression data. Nat Commun. 2013;4:2612.
15. Newman AM, Liu CL, Green MR, Gentles AJ, Feng W, Xu Y, Hoang CD, Diehn M, Alizadeh AA. Robust enumeration of cell subsets from tissue expression profiles. Nat Methods. 2015;12:453-457.
16. Zeng D, Zhou R, Yu Y, Luo Y, Zhang J, Sun H, Bin J, Liao Y, Rao J, Zhang Y, Liao W. Gene expression profiles for a prognostic immunoscore in gastric cancer. Br J Surg. 2018;105:1338-1348.
17. Ali HR, Chlon L, Pharoah PD, Markowetz F, Caldas C. Patterns of Immune Infiltration in Breast Cancer and Their Clinical Implications: A Gene-Expression-Based Retrospective Study. Plos Med. 2016;13:e1002194-e1002218.
18. Hu J, Zhou L, Song Z, Xiong M, Zhang Y, Yang Y, Chen K, Chen Z. The identification of new biomarkers for bladder cancer: A study based on TCGA and GEO datasets. J Cell Physiol. 2019;234:15607-15618.
19. Berdik C. Unlocking bladder cancer. Nature. 2017;551:S34-S35.
20. Monkkonen T, Debnath J. Inflammatory signaling cascades and autophagy in cancer. Autophagy. 2018;14:190-198.
21. Mowers EE, Sharifi MN, Macleod KF. Functions of autophagy in the tumor microenvironment and cancer metastasis. Febs J. 2018;285:1751-1766.
22. Cho SH, Pak K, Jeong DC, Han ME, Oh SO, Kim YH. The AP2M1 gene expression is a promising biomarker for predicting survival of patients with hepatocellular carcinoma. J Cell Biochem. 2019;120:4140-4146.
23. Babjuk M. Bladder Cancer in the Elderly. Eur Urol. 2018;73:51-52.
24. Roma-Rodrigues C, Mendes R, Baptista PV, Fernandes AR. Targeting Tumor Microenvironment for Cancer Therapy. Int J Mol Sci. 2019;20.
25. Bussard KM, Mutkus L, Stumpf K, Gomez-Manzano C, Marini FC. Tumor-associated stromal cells as key contributors to the tumor microenvironment. Breast Cancer Res. 2016;18:84.
26. Ocana A, Nieto-Jiménez C, Pandiella A, Templeton AJ. Neutrophils in cancer: prognostic role and therapeutic strategies. Mol Cancer. 2017;16:137.
27. Coffelt SB, Wellenstein MD, de Visser KE. Neutrophils in cancer: neutral no more. Nat Rev Cancer. 2016;16:431-446.

28. Ali HR, Chlon L, Pharoah PD, Markowetz F, Caldas C. Patterns of Immune Infiltration in Breast Cancer and Their Clinical Implications: A Gene-Expression-Based Retrospective Study. Plos Med. 2016;13:e1002194.
29. Xie L, Li H, Zhang L, Ma X, Dang Y, Guo J, et al. Autophagy-related gene P4HB: a novel diagnosis and prognosis marker for kidney renal clear cell carcinoma. Aging (Albany NY). 2020;12:1828-1842.
30. Sanchez-Carbayo M, Socci ND, Lozano J, Saint F, Cordon-Cardo C. Defining molecular profiles of poor outcome in patients with invasive bladder cancer using oligonucleotide microarrays. J Clin Oncol. 2006;24:778-789.
31. Yusenko MV, Kuiper RP, Boethe T, Ljungberg B, van Kessel AG, Kovacs G. High-resolution DNA copy number and gene expression analyses distinguish chromophobe renal cell carcinomas and renal oncocytomas. Bmc Cancer. 2009;9:152.
32. Liu H, Ma Y, He HW, Zhao WL, Shao RG. SPHK1 (sphingosine kinase 1) induces epithelial-mesenchymal transition by promoting the autophagy-linked lysosomal degradation of CDH1/E-cadherin in hepatoma cells. Autophagy. 2017;13:900-913.
33. Travelli C, Colombo G, Mola S, Genazzani AA, Porta C. NAMPT: A pleiotropic modulator of monocytes and macrophages. Pharmacol Res. 2018;135:25-36.

Tables

Table 1 Construction of five PDEARGs-based prognostic risk model

Genes	Coefficient	HR	HR.95L	HR.95H	*P*-value
APOL1	-0.0019	0.9981	0.9968	0.9995	0.0058
DIRAS3	0.0775	1.0806	1.0116	1.1543	0.0212
NAMPT	0.0127	1.0128	1.0047	1.0210	0.0019
P4HB	0.0030	1.0030	1.0017	1.0043	0.0000
SPHK1	0.0120	1.0121	0.9979	1.0264	0.0944

HR, hazard ratio; HR.95H and HR.95L, 95% confidence interval.

Table 2 Clinical utility of prognostic model related factors [*t*-value (*P*-value)]

Genes	Age	Gender	Grade	Stage	T	M	N
APOL1	2.602(0.011)	-1.622(0.109)	-1.66(0.115)	2.652(0.010)	1.855(0.068)	2.641(0.031)	3.284(0.001)
DIRAS3	-1.412(0.160)	0.985(0.331)	3.272(0.002)	-2.918(0.004)	-2.442(0.016)	1.283(0.234)	-1.72(0.091)
NAMPT	-0.159(0.874)	1.112(0.272)	4.022(2.157e-04)	-3.063(0.003)	-2.526(0.013)	0.812(0.445)	-1.121(0.266)
P4HB	-1.763(0.081)	0.175(0.862)	2.993(0.008)	-2.112(0.037)	-0.98(0.329)	0.416(0.691)	-2.375(0.020)
SPHK1	-1.269(0.206)	0.635(0.529)	7.326(1.635e-11)	-3.207(0.002)	-3.547(5.201e-04)	0.61(0.552)	-1.364(0.177)
Risk score	-2.244(0.026)	1.6(0.116)	6.294(1.13e-07)	-4.839(3.471e-06)	-3.201(0.002)	0.363(0.724)	-3.001(0.003)

Table 3 The construction of PDEARGs-based systematic prognostic signature

Variables	Coefficient	HR	HR.95L	HR.95H	*P*-value
Gender	-0.5755	0.5624	0.3085	1.0253	0.0603
Stage	0.6253	1.8687	1.2486	2.7968	0.0024
Risk score	0.5276	1.6949	1.2194	2.3558	0.0017

HR, hazard ratio; HR.95H and HR.95L, 95% confidence interval.

Figures

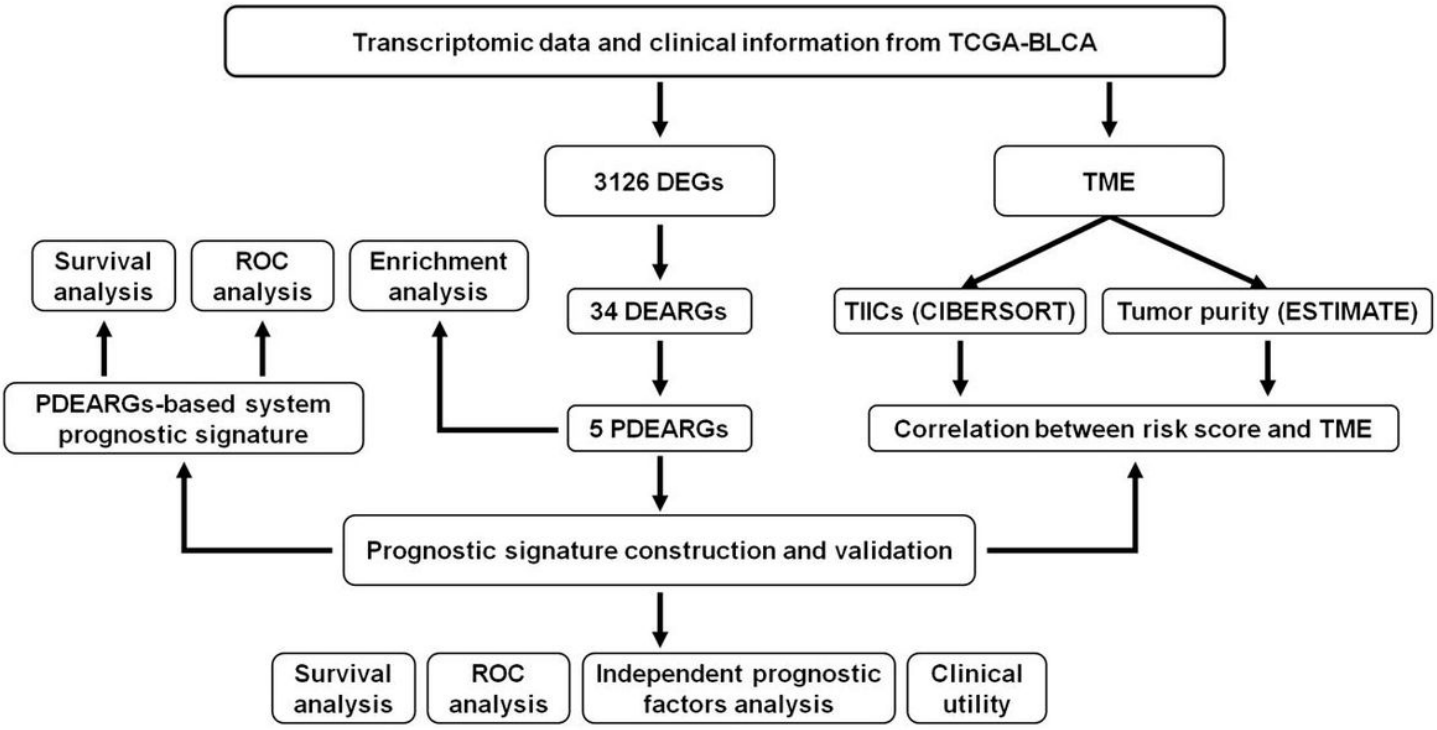

Figure 1

Flow diagram of the present study.

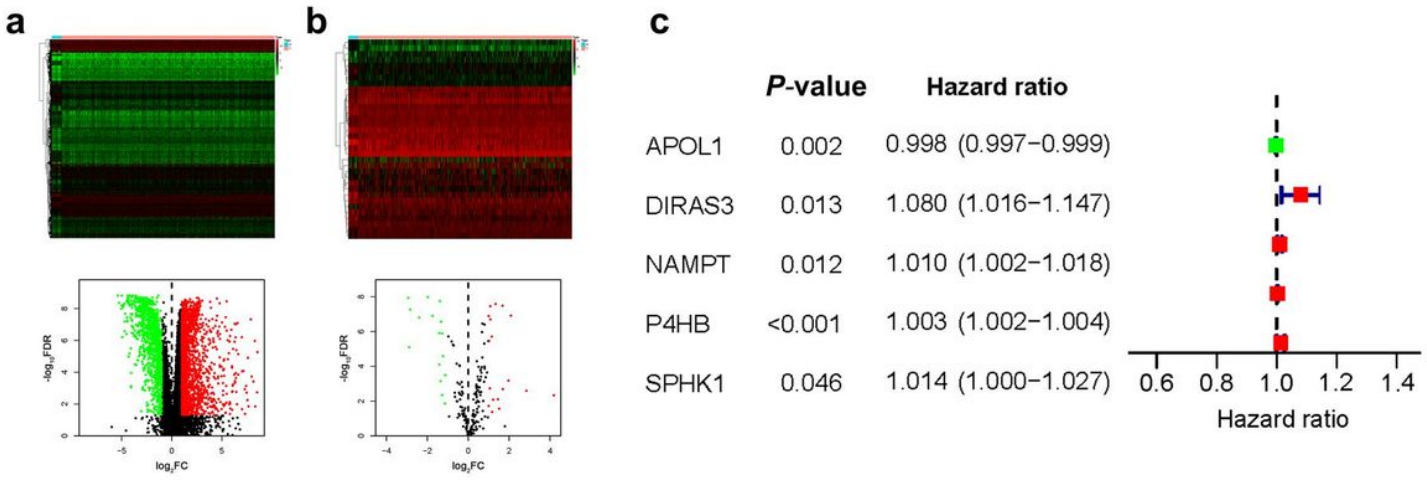

Figure 2

Identification of BLCA specific DEGs, DEARGs and PDEARGs. (a) Heat map and volcano plot of DEGs. (b) Heat map and volcano plot of DEARGs. The green to red spectrum indicates low to high gene expression in heat map; the red, green and black dots represent upregulated, downregulated and unchanged genes in volcano plot, respectively. (c) Forest graph of PDEARGs. The red and green dots represent PDEARGs with hazard ratio > 1 and ≤ 1, respectively.

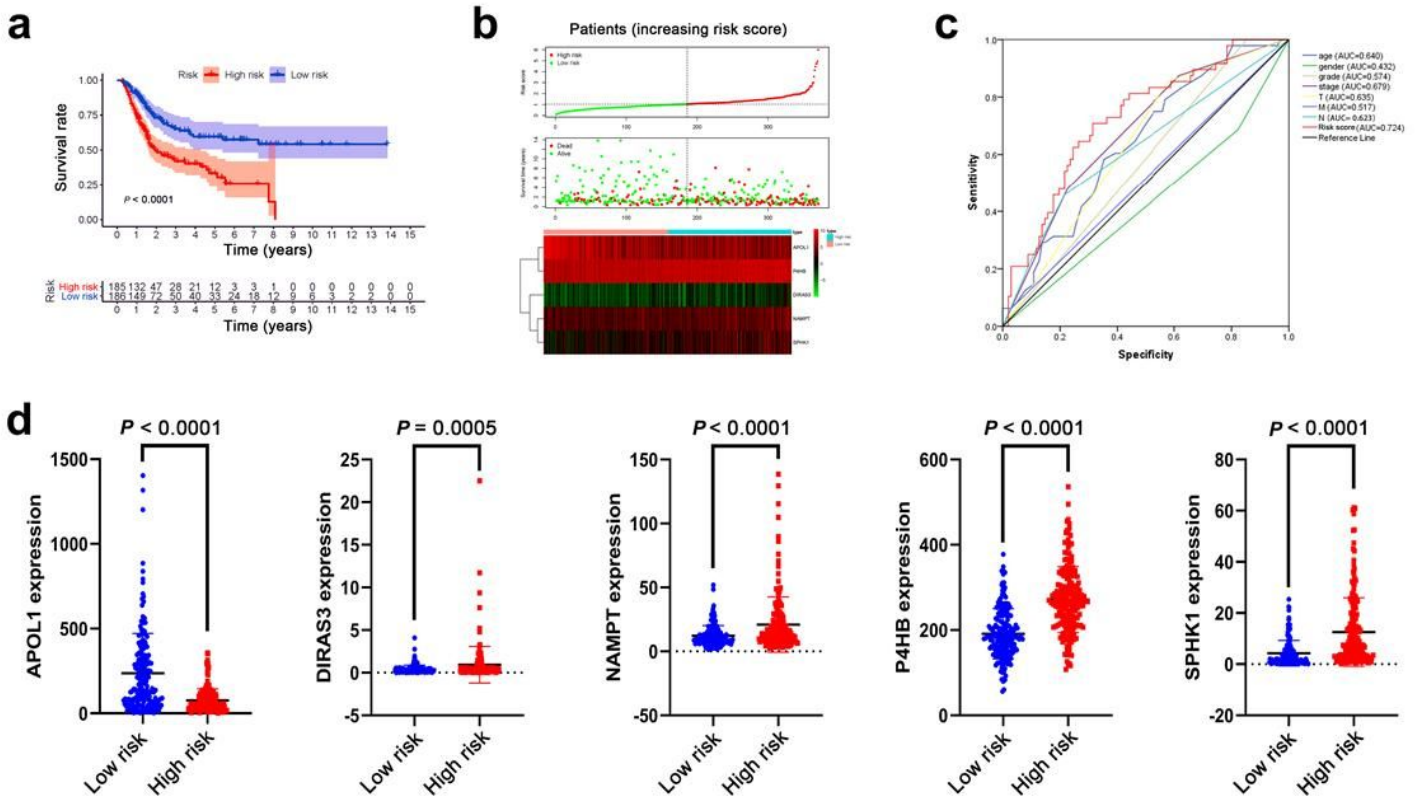

Figure 3

Prognostic value of present risk model. (a) Survival analysis between high-risk and low-risk groups. The 95% confidence interval was shown as a light-colored background around the Kaplan-Meier curve. (b) Risk plot encompassing the distribution of risk score, survival status and the expression of risk genes in each patient. (c) ROC curve analysis of different variables. (d) Expression level of the five selected PDEARGs between low-risk and high-risk group. Data are represented as mean ± SD.

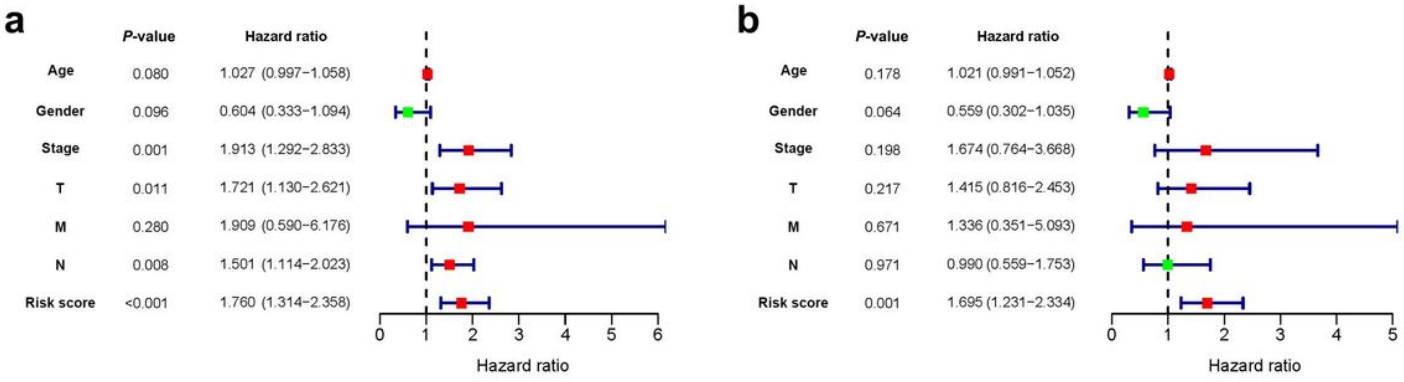

Figure 4

Univariate and multivariate Cox regression analysis. (a) Univariate Cox regression analysis to identify prognosis associated factors. (b) Multivariate Cox regression analysis to assess independent prognostic factors. The red and green dots represent variables with hazard ratio > 1 and ≤ 1, respectively.

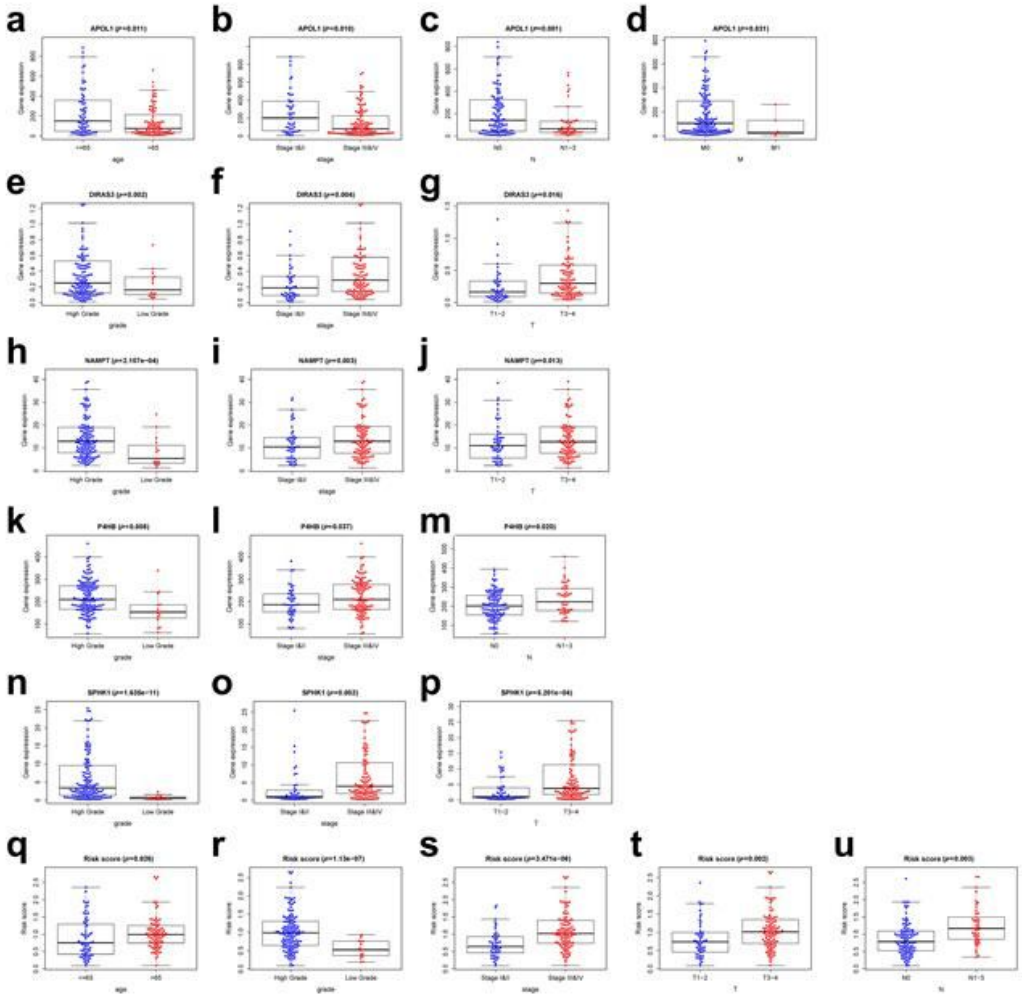

Figure 5

Relationship between prognostic model related factors and clinical variables. (a-d) APOL1 and clinical variables. (e-g) DIRAS3 and clinical variables. (h-j) NAMPT and clinical variables. (k-m) P4HB and clinical variables. (n-p) SPHK1 and clinical variables. (q-u) Risk score and clinical variables. Box plots with P < 0.05 are shown.

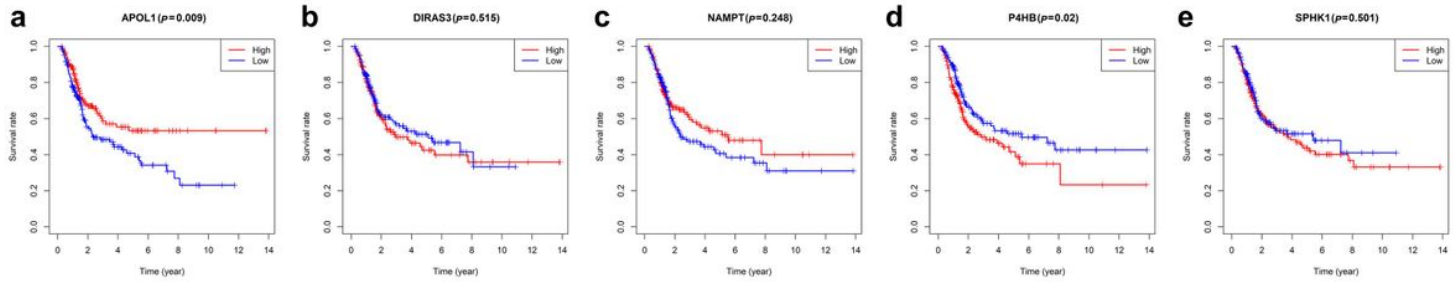

Figure 6

Survival analysis of prognostic model related genes. Kaplan-Meier curve of patients with different expression level of APOL1 (a), DIRAS3 (b), NAMPT (c), P4HB (d), SPHK1 (e). Median expression level was used as the cut-off value. Red line and blue line represent high expression and low expression group, respectively.

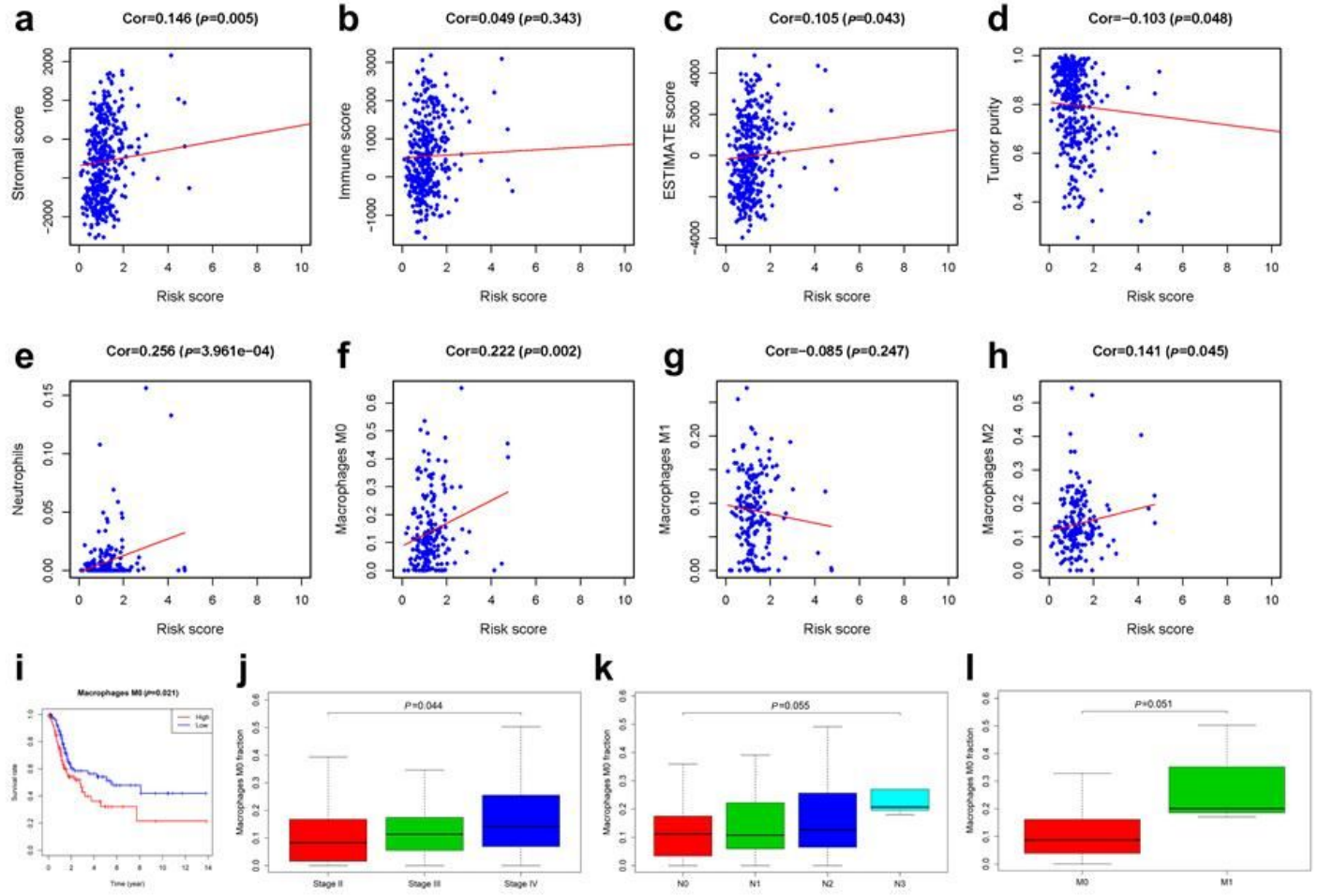

Figure 7

The correlation between risk score and TME. (a) Risk score and stromal score. (b) Risk score and immune score. (c) Risk score and ESTIMATE score. (d) Risk score and tumor purity. (e) Risk score and neutrophils. (f) Risk score and macrophage M0. (g) Risk score and macrophage M1. (h) Risk score and macrophage M2. (i-l) Macrophage M0 and clinical variables.

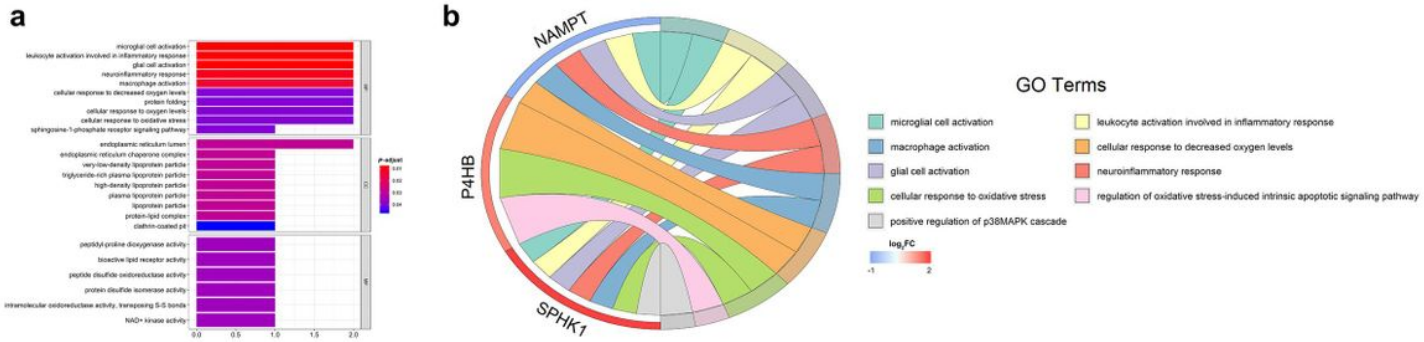

Figure 8

GO enrichment analysis of PDEARGs. (a) Bar plot of enriched GO terms. (b) Chord plot of enriched GO terms. FDR < 0.05 was considered statistically significant.

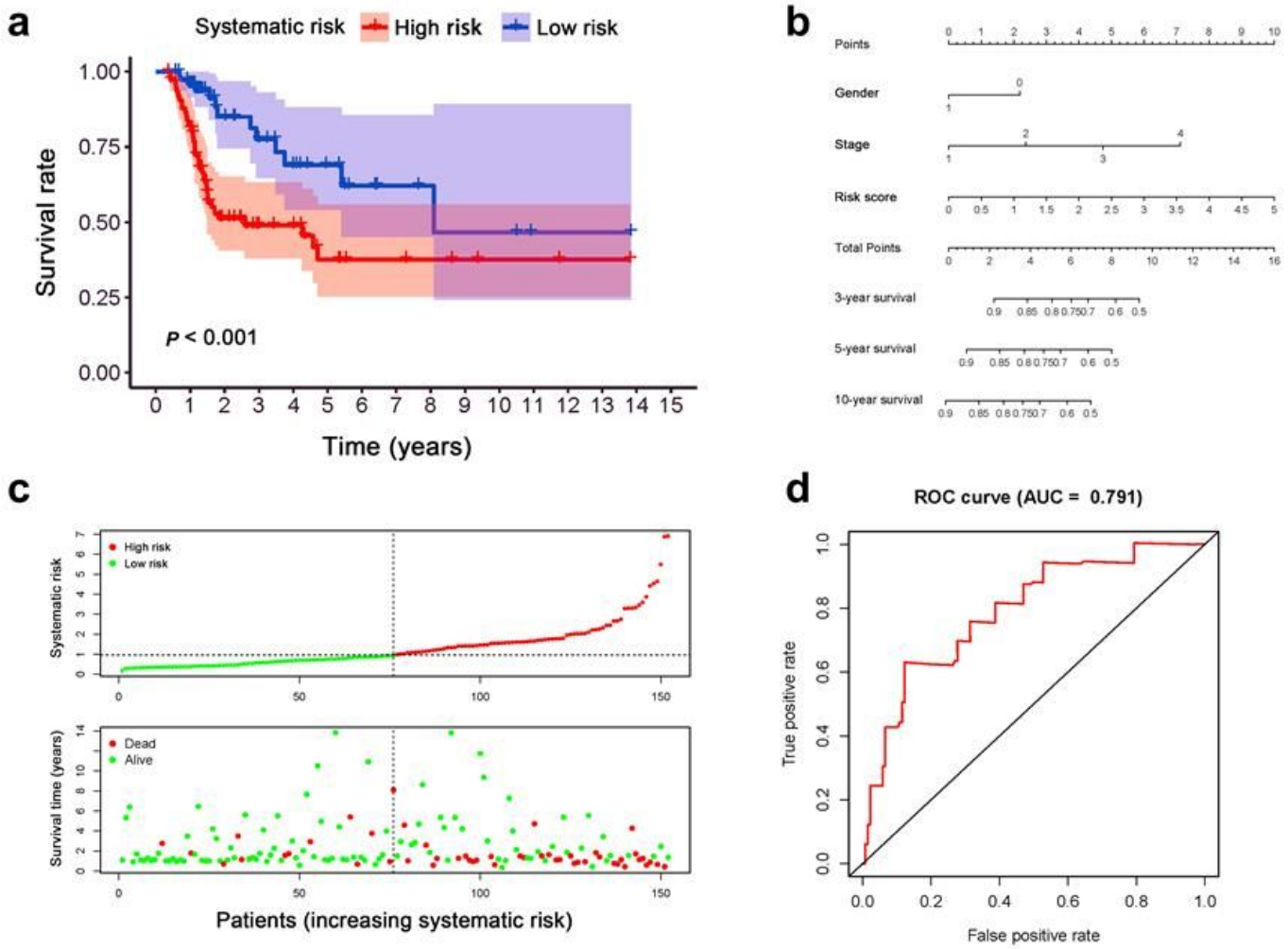

Figure 9

The construction and validation of PDEARGs-based systematic prognostic signature. (a) Survival analysis between two groups with different systematic risk. The 95% confidence interval was shown as a light-colored background around the Kaplan-Meier curve. (b) Nomogram of the systematic prognostic signature. (c) Risk plot encompassing the distribution of systematic risk and survival status of each patient. (d) ROC curve analysis of systematic risk.